CHAPTER V: EXPERIMENTAL RESEARCH PERFORMED AT THE UNIVERSITY OF LIEGE AND SIMULATIONS BY SAFIR

V.1 Experimental programme and its objectives

A research project entitled: « Etude du comportment à froid et sous conditions d'incendie de colonnes réalisées en tubes métalliques remplis de béton auto-plaçant" (Steel hollow section columns filled with self compacting concrete at normal temperatures and under fire conditions) has been realized in Belgium with the financial support of the Belgian FNRS-FRFC (Fonds National de la Recherche Scientifique – National Funds for Scientific Research). In this study, steel hollow section columns filled with self compacting concrete has been investigated theoretically and experimentally.

In this type of profile, concrete is generally reinforced by classical steel bars. An alternative consists in replacing these bars by another tube or a H profile placed inside the external tube. When the space between the two profiles becomes narrow, the filling by traditional concrete becomes impossible, but it is possible to envisage this filling by using self-compacting concrete (SCC). Due to the choice of appropriate additives, a remarkable fluidity can be obtained for this type of concrete, allowing the filling of narrow spaces without any vibration, provided sufficiently small aggregates are provided.

This research is carried out at the Université Libre de Bruxelles (ULB)- Belgium and at the University of Liège (ULg)- Belgium.

At ULB, the software FLOW3D developed at LCPC in Paris was used to model the flow of concrete in the columns. The type of concrete was chosen on the basis of these simulations.

At ULg, numerical simulations were done to investigate the behaviour of steel hollow section (SHS) columns filled with self-compacting concrete at room temperatures and under fire conditions. The results of these simulations have been used to defined the experimental programme at elevated temperatures. A simplified method for predicting the fire resistance of CFSHS columns was then proposed (see chapter VI)

Experiments have been made in both normal temperature condition and fire conditions. 20 column tests were realized:

- 10 tests under normal temperature conditions at the University of Brussels (ULB)
- 10 tests under fire conditions at the University of Liège (ULg)

5 profiles were used, each tested twice.

Before concreting, thermocouples were installed in the columns to be tested under fire condition were installed thermocouples at ULg and these elements were transported to ULB. All columns were concreted at ULB. The tests on materials were performed at ULB also.

At the time this chapter is written, no information is available on the test results on columns under normal temperature conditions performed at ULB. Therefore, this chapter described the fire tests performed at University of Liège.

V.2 Test specimens

V.2.1 Dimensions

The length of all columns is 3310 mm from end plate to end plate. There are five different cross sections named profile 1 to profile 5, each profile being tested twice. They are named FRFC 1A, FRFC 1B, FRFC 2A, FRFC 2B… FRFC 5A, FRFC 5B.

Column FRFC 1A and FRFC 1B are identical but the values of the compressive load are different. It is the same for the couples FRFC 2A-2B and FRFC 5A-5B.

The cross-section of columns FRFC 3A and FRFC 3B are identical but column FRFC 3A will be tested with the eccentric compressive load creating buckling around the major axis while column FRFC 3B will be tested for buckling around the minor axis. In this case, the fire resistance will be much lower. Therefore, column FRFC 3B was painted using intumescent paint 7H-960 C-THERM HB. The thickness of the painting layer is 465 μm theoretically (~ 0.5 mm). This value was chosen according to the indications of the painting manufacturer for pure external steel hollow section column (without concrete core) in order to reach a fire resistance of 30 minutes. Of course, a longer duration of fire resistance is expected for column FRFC 3B because of the presence of the concrete core.

The same is valid for the couple FRFC 4A- 4B but the thickness of the painting layer for column FRFC 4B is theoretically 1968 μm (~ 2 mm). This value is for pure external steel hollow section column (without concrete core) in order to reach a fire resistance of 60 minutes.

Profile 1 (Figure V-1):
External profile: Circular hollow section 219.1 x 5
Internal profile: Circular hollow section 139.7 x 10
Concrete cover thickness: ~ 35 mm

Profile 2 (Figure V-2):
External profile: Circular hollow section 219.1 x 5
Internal profile: Square hollow section 120 x 10
Concrete cover thickness: from 26 to 45 mm

Profile 3 (Figure V-3):
External profile: Circular hollow section 219.1 x 5
Internal profile: H profile HEB120

Profile 4 (Figure V-4):
External profile: Square hollow section 200 x 5
Internal profile: H profile HEB120

Profile 5 (Figure V-5):
External profile: Circular hollow section 273 x 5
Internal profile: Circular hollow section 168.3 x 10
Concrete cover thickness: ~ 47 mm

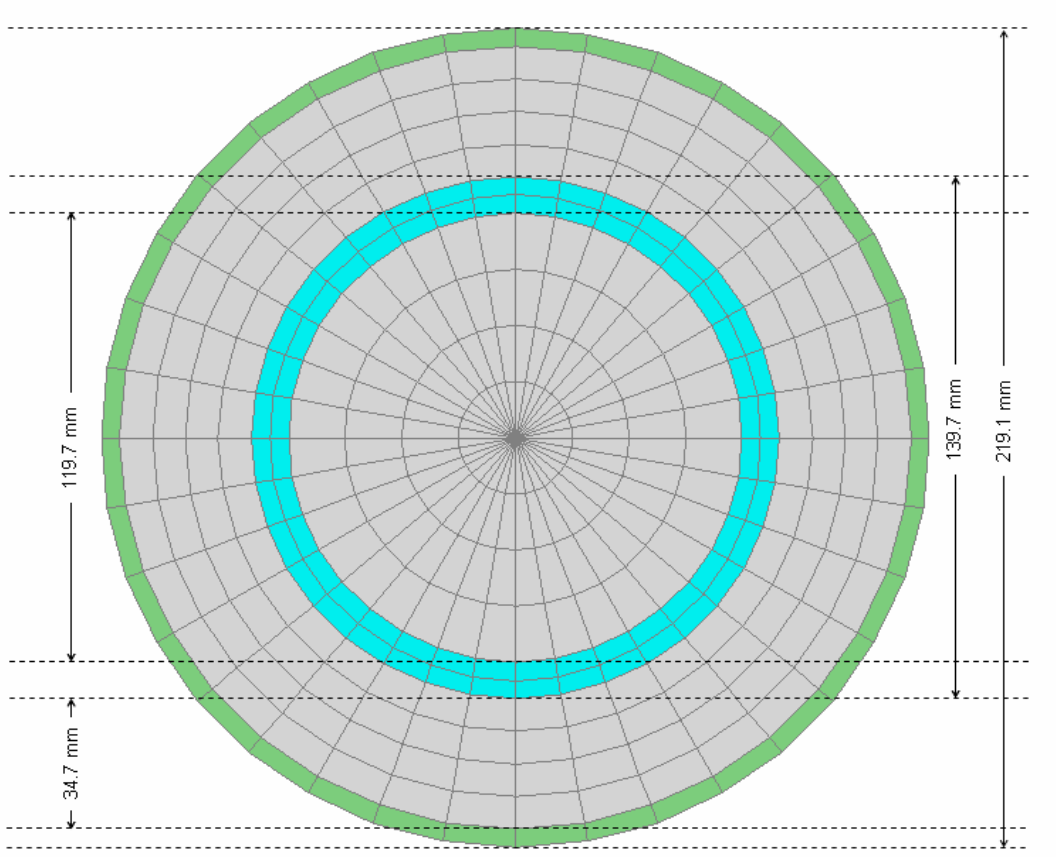

Figure V-1. Cross-section of profile 1

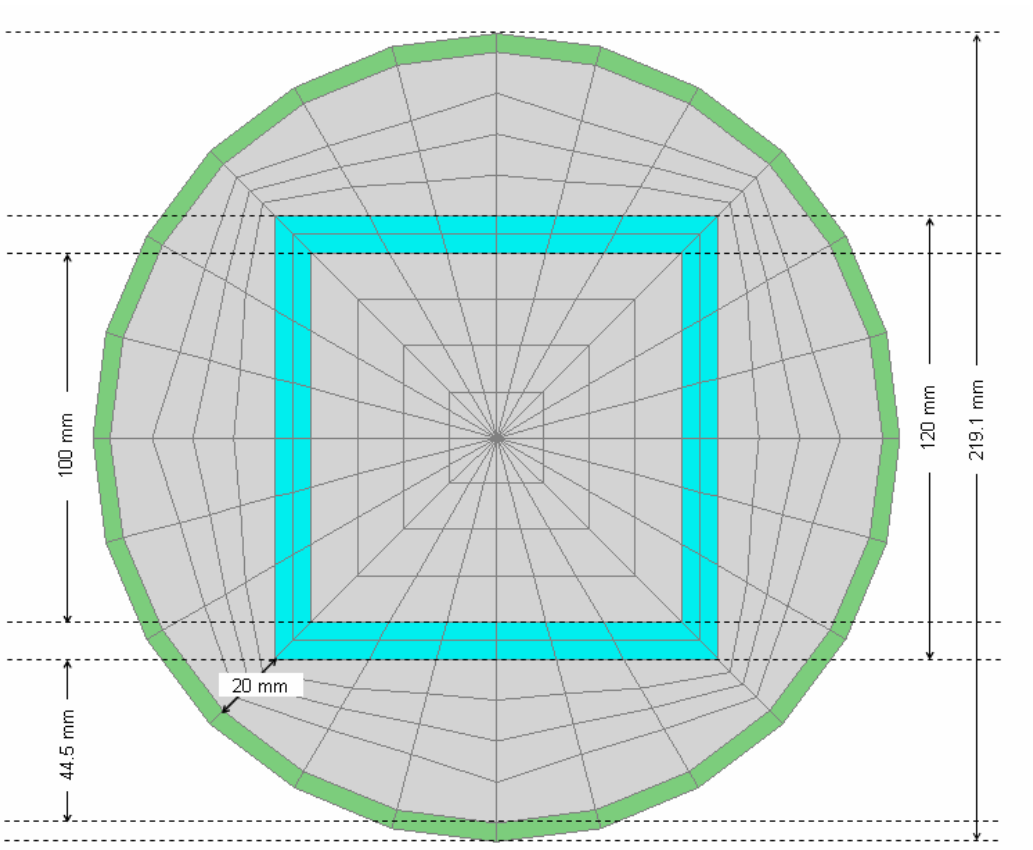

Figure V-2. Cross-section of profile 2

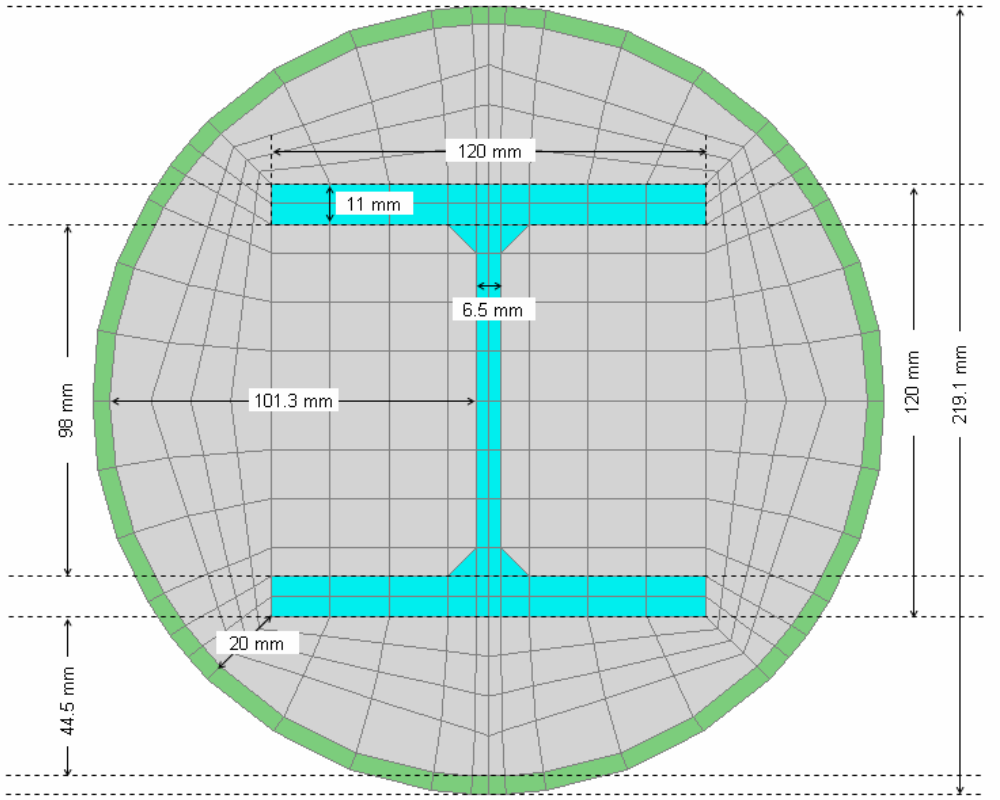

Figure V-3. Cross-section of profile 3

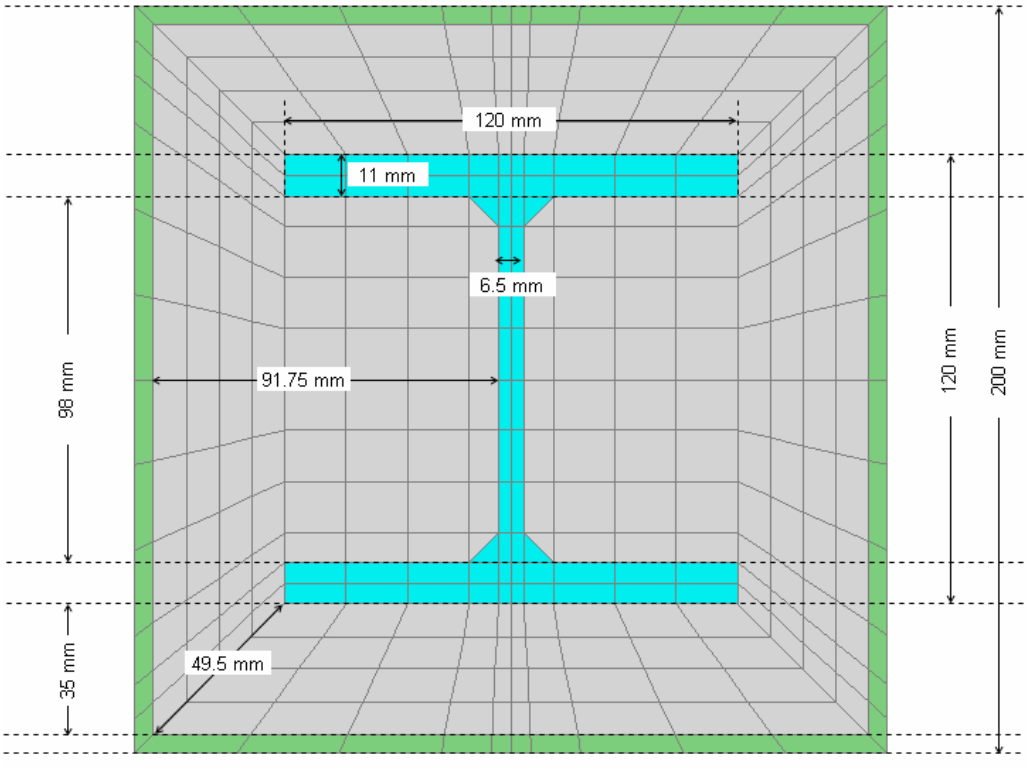

Figure V-4. Cross-section of profile 4

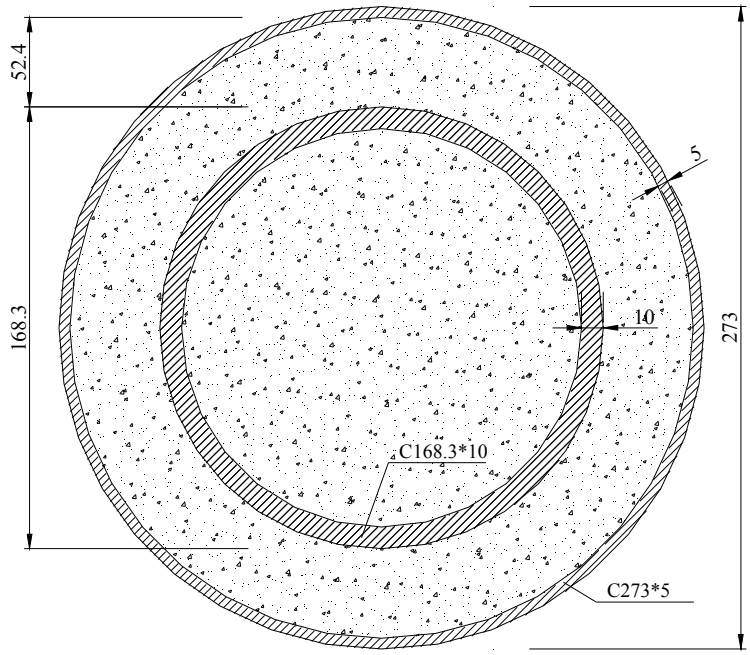

Figure V-5. Cross-section of profile 5

An additional test on two identical short columns (called profile 6-Figure V-6) with the cross-section being the same as for profile 5, except that the internal profile is empty (no concrete infill). This configuration allows the installation of water pipes and electrical cables inside the composite column. The column height was 500 mm. This test was only performed for verifying the thermal transfer in the cross-section. No load was applied.

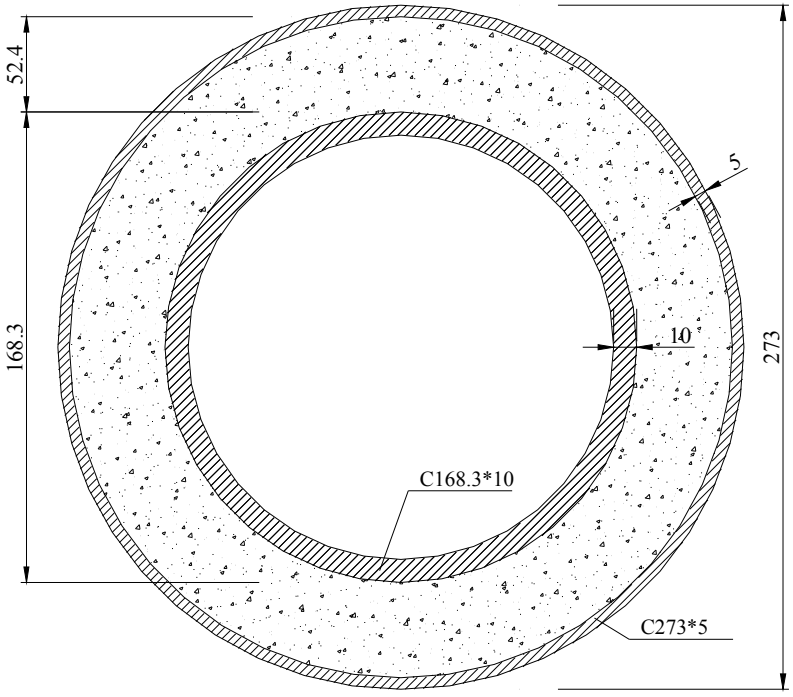

Figure V-6. Cross-section of profile 6

V.2.2 Materials

Steel:
The quality of hollow section tubes is S355 J2H EN 10210. The steel grade of the HEB profiles is also S355.

Concrete:
The premix Sikacrete 08-SCC was used. 2.75 liters of water are added to one bag of Premix SIKA of 25 kg. With this proportion a concrete class C25/30 can be expected.

V.2.3 Fabrication

Steel column:

The steel profiles were fabricated by cutting the sections to appropriate lengths. The bottom end plates were then welded to one end of the sections. Centering and perpendicularity of the end plates were given special attention. The components of the columns were dimensioned so that their length was 3310 mm, including the plate thickness (Figure V-7).

Eight steam vent holes were drilled near the ends of the columns. Two holes to accommodate the thermocouple cables were drilled near one face of the tube, this face being then defined to be the "bottom" face with respect to its position within the test furnace.

Concrete placement:

Before casting the real specimens, a column with the external steel wall replaced by a plastic wall was concreted to check if the workability of SCC was good enough for the filling without the vibration. 7 days after concreting, the plastic wall was cut out and the concrete inside was observed. It has been verified that all space in the section was filled with SCC.

Thermocouples:

Type K- chromel-alumel thermocouples, with a thickness of 0.5 mm, were used for measuring temperatures in concrete, internal steel profile and external steel tube at several locations in different cross sections of the columns. Typical locations of thermocouples are shown in Figure V-8. The detailed locations of thermocouples in all tests can be found in Appendix 2

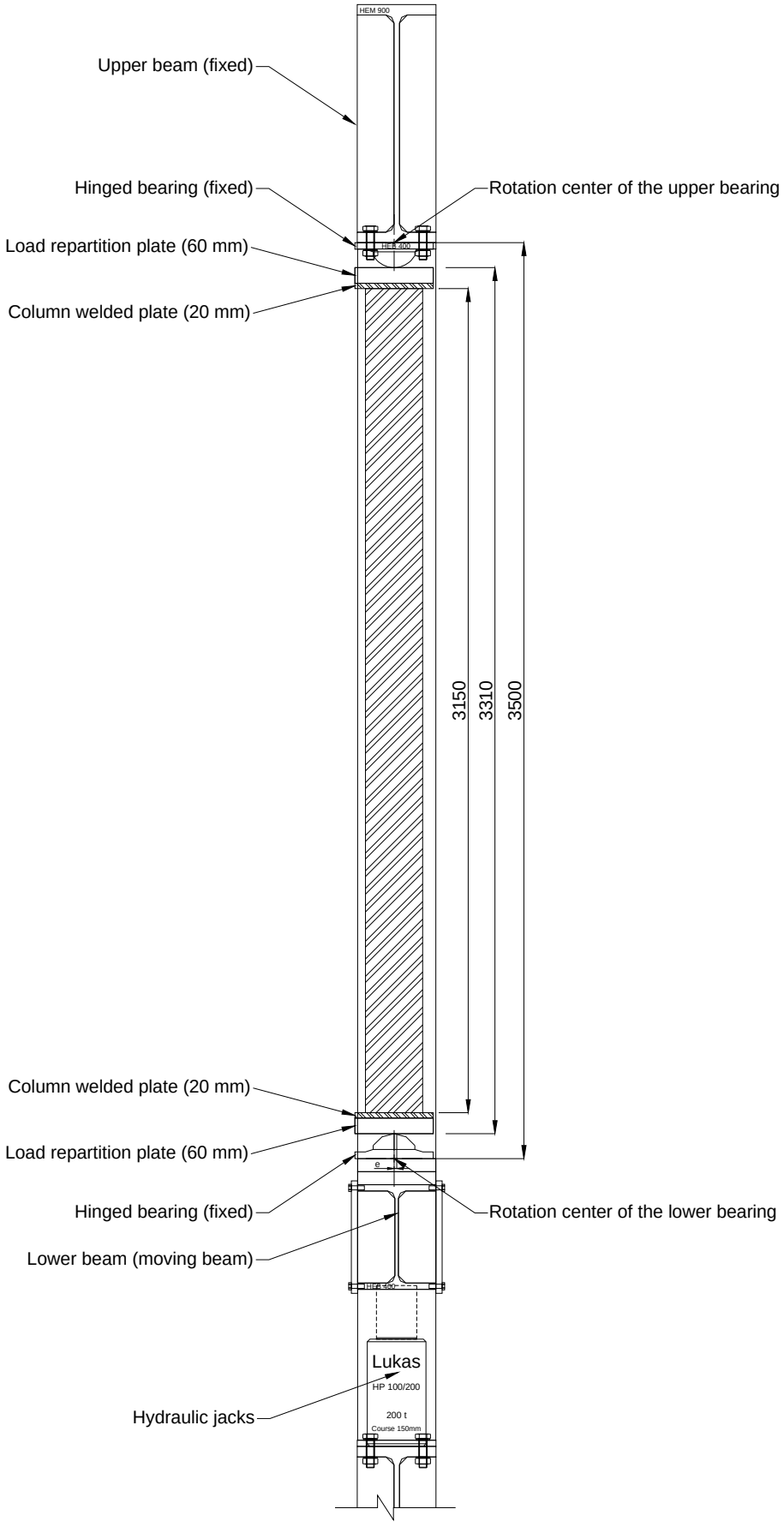

Figure V-7. Testing device for the columns

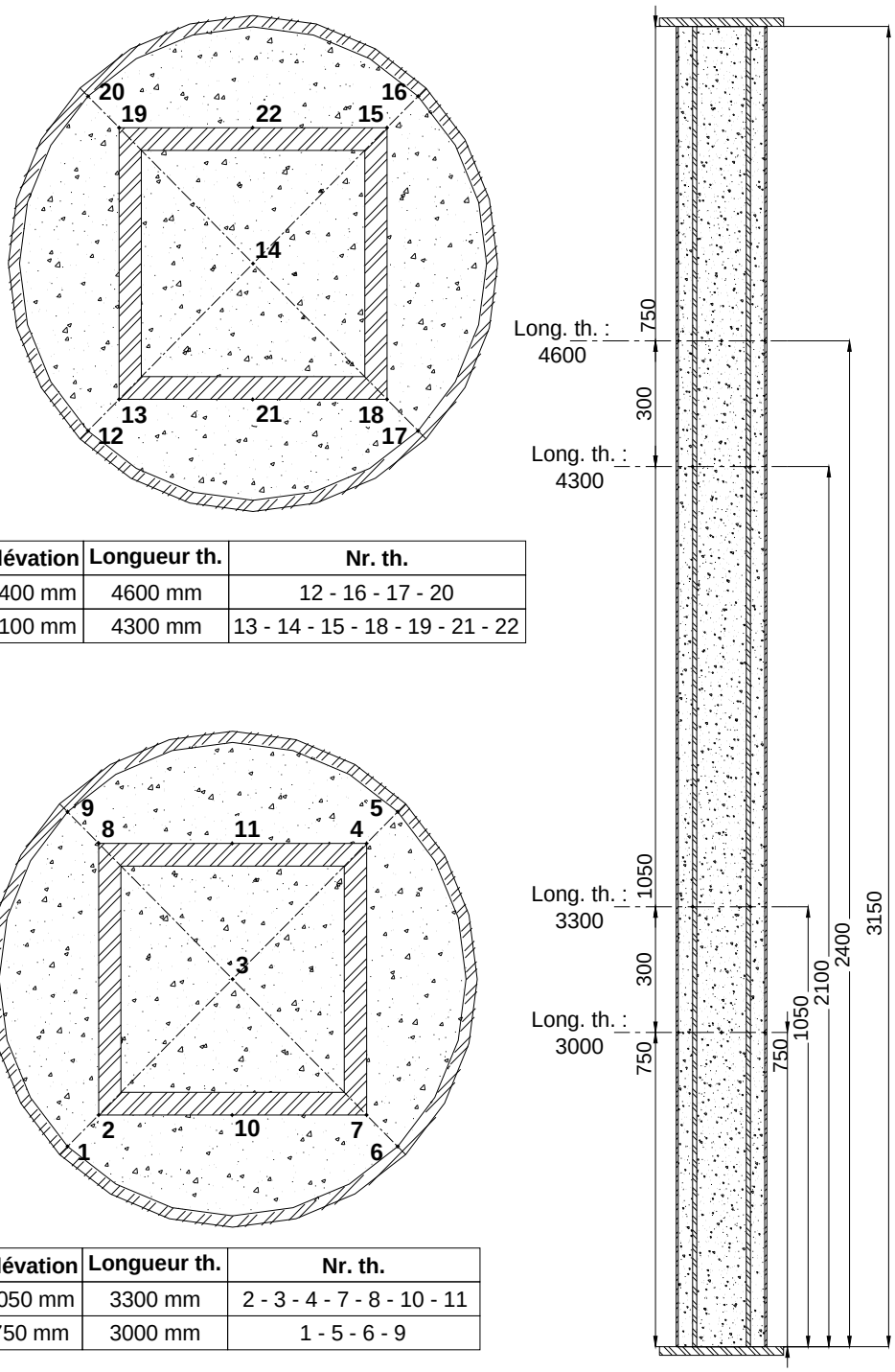

Elévation	Longueur th.	Nr. th.
2400 mm	4600 mm	12 - 16 - 17 - 20
2100 mm	4300 mm	13 - 14 - 15 - 18 - 19 - 21 - 22

Elévation	Longueur th.	Nr. th.
1050 mm	3300 mm	2 - 3 - 4 - 7 - 8 - 10 - 11
750 mm	3000 mm	1 - 5 - 6 - 9

Figure V-8. Location of thermocouples in columns

V.3 Tests on material properties

All these tests have been made at the University of Brussels

V.3.1 Steel strength

Tensile tests were performed according to EN 10002-1 to determine the stress-strain relationship. The yield strength, ultimate strength and elastic modulus of the material are given in Table V.1. As no sample of the tube C 273*5 was left, the properties of steel tube C 273*5 are assumed to be the same as those of the tube C 219.1*5.

Profile	Yield strength (MPa)	Ultimate strength (MPa)	Elastic modulus (MPa)
Tube S 200*200*5	510	550	203200
Tube S 120*120*10	349	521	191200
Tube C 219.1*5	420	538	214500
Tube C 168.3*10	333	525	170700
Tube C 139.7*10	340	510	244200
Profile HEB 120	375	587	191300

Table V.1 Mechanical properties of the steel

It can be observed that there is a big scatter of the experimental values for the yield strength of the tubes: one value is much higher than the characteristic value (355 MPa), one is higher, and three are lower.

There is also a larger variation for the elastic modulus (from 170700 MPa to 244200 MPa).

V.3.2 Cube compressive strength of concrete

When concreting the specimens, concrete cubes 120 mm were made to test the concrete strength. The compressive strength of the cubes at 28 days is 41.5 MPa. By modifying this strength in order to get the strength of cylinder of 150 * 300 mm at an age of more than 3 months, the value of 35 MPa is obtained. This value is chosen in simulations predicting the behaviour of test columns.

V.3.3 Water content of concrete

From concrete mix two cylinders with diameter 112.5 mm and height 217.5 mm were casted. The mean water content in concrete was determined by oven drying technique according to European standard EN 1363-1. More than 3 months after concreting, the values of water content in concrete are 6.3% and 6.15% in weight. The value 6% is chosen in simulations.

V.4 Test apparatus

The fire tests were performed at the fire testing laboratory of the University of Liege-Belgium. The tests were carried out in accordance with EN 1365-4

V.4.1 Loading device

The load is produced by hydraulic jacks with total capacity of 3000 KN. The jacks are located at the bottom of the furnace chamber. Columns are supported by a fixed beam at the top end

and a moving beam at the bottom end (Figure V-7). The moving beam is supported by the hydraulic jacks so it can move vertically when the jacks produce load.

V.4.2 Furnace chamber

The vertical furnace is 3250 mm wide and 3250 mm high. Fire resistance tests are carried out in accordance with standard NBN 713-020.
At the origin furnace was built to test only vertical separating elements. Therefore a new part was built and attached to the new part (Figure V-10). The new part has not got burners. There are 10 burners in the old part of the furnace chamber. The total capacity of the burners is 2500 kW. The burners can be adjusted from level 1 to level 10, which allows reaching easily the desired temperature in the furnace chamber. But there thermal gradients are expected between the new part and the old part of the furnace, which will be confirmed by experimental results

V.4.3 Instrumentation

The furnace temperatures are measured by thermoplates which are located about 150 mm from the test specimen, at various heights. The temperatures measured by the thermoplates are averaged automatically and the average temperature is used as the criterion for controlling the furnace temperature. The locations of the thermoplates are shown in Figure V-10

In some tests (FRFC 1B, FRFC 2A, FRFC 3A, FRFC 3B, FRFC 4A, FRFC 5B), two strain gauges were attached for measuring the strains at two points situated opposite on the external tube at middle height of the column. The location of the strain gauges is shown in Figure V-9. These gauges are used to measure the deformation of the column in the loading stage (at room temperature). Using the opposite values, it is possible to predict the curvature of the column, and assuming the deflection to be represented by a sin function, it is also possible to predict the deflection at mid-height, and to compare it with the values measured by the wire (see hereafter). In the test FRFC 3A, the strain gauges were protected from heating by ceramic fiber layers (Figure V-11). With this protection it is intended to measure the strains during the fire test. It is expected that the strain gauges can be protected from fire in the first 5 or 10 minutes.

The transversal displacement at mid-height of the columns was evaluated using a wire going outside of the furnace. A transducer measured the transversal displacement of the wire. A thermocouple was attached to the wire for measuring the temperature during the fire test and thus calculating the thermal elongation of the wire. During the first test FRFC 1A, the wire was a steel bar. But in this test the steel wire showed large deformations, which led to unreliable measurement values. Therefore the steel wire was replaced by a ceramic one for all the next tests. The ceramic wire does not deform like the steel wire and has a smaller coefficient of thermal elongation. This coefficient was measured during a fire test of another project. The result is shown in Figure V-12.

The axial (vertical) displacement of the columns was determined by measuring the displacements at two points near the end of the moving beam that supports the columns. The vertical displacement of the column is the mean value of the two measured values.

After the first tests, it was found that the measured displacements by transducers do not agree with the displacements calculated from strain measurements when the load is applied. It was suspected that the bottom beam moves laterally and rotates during the test. In order to check this, two displacement measurements were added in the test FRFC 5B: central vertical and lateral displacement of the moving beam.

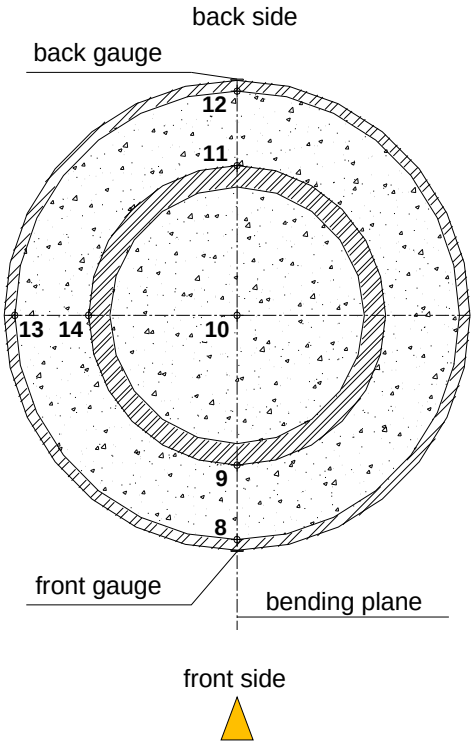

Figure V-9. Location of the strain gauges in the column

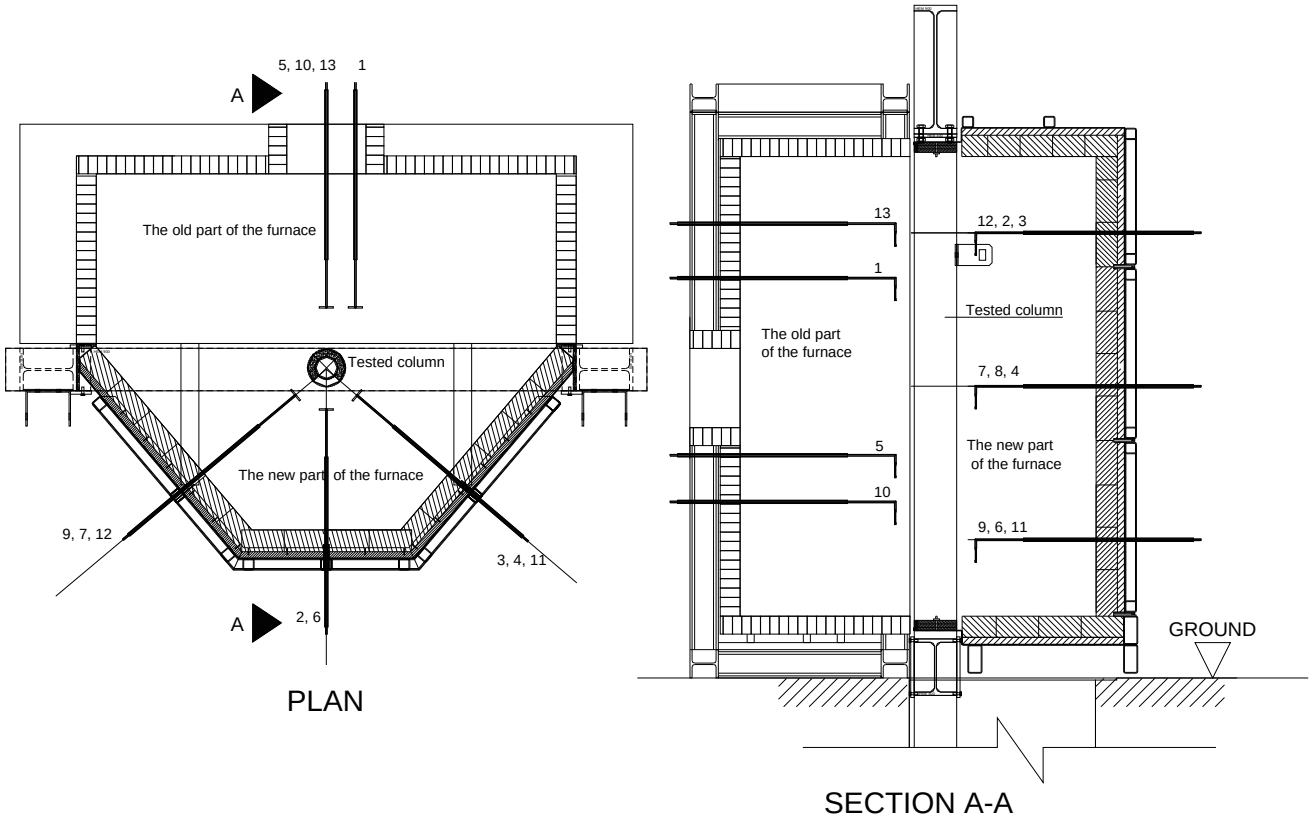

Figure V-10. Location of thermoplates in the furnace

Figure V-11. Fire protection of the strain gauges of the test FRFC 3A

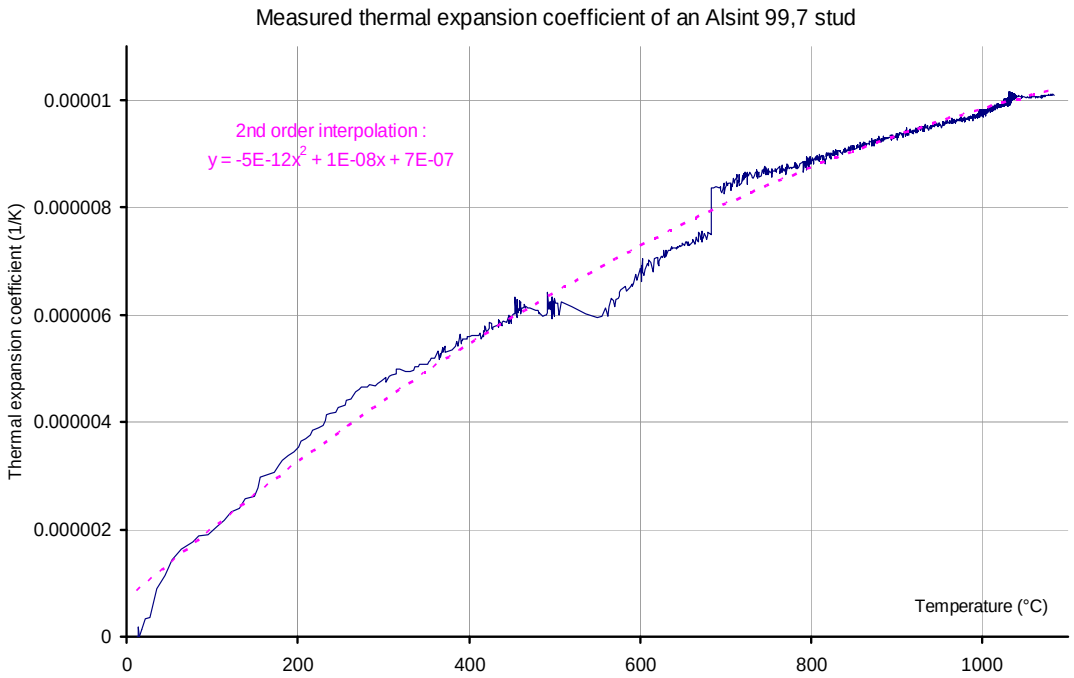

Figure V-12. Measured thermal expansion coefficient of the ceramic wire used for measuring the transversal displacement at midheight of the columns.

V.5 Test conditions and procedures

The columns were installed in the furnace by securing the end plates to the plates of the bearings. The bearings were bolted to a loading head at the top and to the plate of the main hydraulic jack. In all cases, the end conditions were hinged. These hinges are rolls so that lateral displacements of the column have to be perpendicular to the furnace.

V.5.1 Assembly / Loading

All columns were subjected to a load situated between 30% and 50% the ultimate load at room temperature. The material properties and the loads of the columns are detailed in Table V.2. As will be shown in chapter 6, the boundaries for the load ratio are approximately 0.2 and 0.6. Instead of making two similar tests with a load ratio of 0.4, for tests 1,2 and 5 the value 0.3 and 0.5 has been adopted, which means a rather low and a rather high value. On the other hand, for test 3 and 4, the test conditions are different (minor or major axis, use or not of intumescent paint), and the mean value of 0.4 has been adopted.

Test	External steel profile		Internal steel profile		Ultimate load at normal temp *		Test load in fire		Load ratio
number	Elastic modulus	Yield strength	Elastic modulus	Yield strength	Load	Eccentricity	Load	Eccentricity	
	(MPa)	(MPa)	(MPa)	(MPa)	Nu (KN)	e (mm)	Nfi (KN)	e (mm)	Nfi/Nu
Profile 1A	192000	420	210000	340	3000 (2443)**	0 (10)**	733	0	0.24 (0.3)**
Profile 1B	192000	420	210000	340	2253	15	1126	15	0.50
Profile 2A	192000	420	191200	349	2294	15	688	15	0.30
Profile 2B	192000	420	191200	349	2489	10	1244	10	0.50
Profile 3A	192000	420	191000	375	2365	10	946	10	0.40
Profile 3B	192000	420	191000	375	2241	10	896	10	0.40
Profile 4A	203000	510	191000	375	2943	10	1177	10	0.40
Profile 4B	203000	510	191000	375	2809	10	1124	10	0.40
Profile 5A	192000	420	171000	333	3995	10	1199	10	0.30
Profile 5B	192000	420	171000	333	3995	10	1998	10	0.50

Table V.2 Structural properties of tested columns

* The ultimate load at normal temperature was predicted using SAFIR simulation by assuming that the initial deformation shape of the columns is a semi-sine curve with maximum deflection of L/500.

* There has been some discussion about the value to be adopted for the load eccentricity. For the first test, no eccentricity was applied; but it was found that the development of buckling was not very clear. For test 2 and 3, the value 15 mm was adopted, but this appeared to be too much for columns with a rather small cross-section. Therefore an eccentricity of e = 10 mm was adopted for the last 7 tests, this value being considered as an additional incidental eccentricity.

* The ultimate load at normal temperature of the test FRFC 1A was calculated in two cases: with no eccentricity of loading and with an eccentricity of 10 mm (the value in parentheses).

V.5.2 Fire exposure

During the test, the columns were exposed to heating controlled in such a way that the average temperature in the furnace followed, as closely as possible, the ISO 834 standard temperature-time curve. This curve is given by following equation:

$$T = 345.\log_{10}(8t+1)+T_0$$

where t is the time (minutes), T_0 is the initial furnace temperature (°C) and T is the furnace temperature at time t

During the test, temperatures in the furnace and in the column were measured at the locations described earlier.

V.5.3 Recording of results

Temperature readings were taken at each thermocouple location at intervals of 15 seconds. The vertical and transversal displacements of the column were monitored throughout each test. The columns were considered to fail when the vertical displacement curve started to go down steeply. At that moment, the test had to be stopped quickly in order to avoid damage in the furnace.

V.6 Test results

They are presented in Table V.3. Only brief results and observations are given here. The detailed descriptions are given in Appendix 2.

	Ultimate load at normal temperatu		Test load in fire		Load ratio	Tested
Test number	Load	Eccentricity	Load	Eccentricity		fire resistance
	Nu (KN)	e (mm)	Nfi (KN)	e (mm)	Nfi/Nu	Rt (minute)
Profile 1A	3000 (2443) *	0 (10)*	733	0	0.24 (0.3)*	86
Profile 1B	2253	15	1126	15	0.50	22
Profile 2A	2294	15	688	15	0.30	65
Profile 2B	2489	10	1244	10	0.50	43
Profile 3A	2365	10	946	10	0.40	56
Profile 3B (with painting)	2241	10	896	10	0.40	64
Profile 4A	2943	10	1177	10	0.40	39
Profile 4B (with painting)	2809	10	1124	10	0.40	79
Profile 5A	3995	10	1199	10	0.30	104
Profile 5B	3995	10	1998	10	0.50	35

Table V.3 Tested fire resistances of the columns

V.6.1 Test FRFC 1A

Tested fire resistance: 86 minutes
Temperatures: Figure A2.4 - Appendix 2
Axial deformation: Figure A2.6- Appendix 2
Lateral deflection at midheight: Figure A2.7- Appendix 2
Observations: The column failed due to the overall buckling toward the old part of the furnace (Picture A2. 1). No local buckling of the external steel tube was observed. Temperatures readings from a thermocouple (Th6) could not be considered because they differ much from the average temperatures of other thermocouples at the same corresponding locations. In the last 15 minutes of the fire test, the temperatures at the external steel tube and at the center of the concrete core decreased (Figure A2.4) while the furnace temperature still increased (Figure A2.3). Measured temperatures at the internal steel profile (Th7 and Th14) increased rapidly in the last 15 minutes of the fire test (Figure A2.5).

V.6.2 Test FRFC 1B

Tested fire resistance: 22 minutes
Temperatures: Figure A2.10- Appendix 2
Axial deformation: Figure A2.11- Appendix 2
Lateral deflection at midheight: Figure A2.12- Appendix 2
Observations: The column failed due to the buckling toward the old part of the furnace (Picture A2.2). A small mark of local buckling of the steel tube is observed at the middle height of the column. But the local buckling deformation is not very clear so it can be assumed that the fire resistance is not affected much by that local buckling

V.6.3 Test FRFC 2A

Tested fire resistance: 65 minutes
Temperatures: Figure A2.17 and Figure A2.18- Appendix 2
Axial deformation: Figure A2.19- Appendix 2

Lateral deflection at midheight: Figure A2.20- Appendix 2
Observations: The column failed due to buckling toward the old part of the furnace. In some periods of the test, temperatures readings from three thermocouples (Th4, Th16, and Th17) were not reliable because they differed much from the average temperatures of other thermocouples at the same corresponding locations.

V.6.4 Test FRFC 2B

Tested fire resistance: 43 minutes
Temperatures: Figure A2.22 and Figure A2.31- Appendix 2
Axial deformation: Figure A2.24- Appendix 2
Lateral deflection at midheight: Figure A2.33- Appendix 2
Observations: The column failed due to overall buckling toward the old part of the furnace. No local buckling of the external steel tube was observed. In some periods of the test, temperatures readings from two thermocouples (Th1 and Th6) were not reliable because they differed much from the average temperatures of other thermocouples at the same corresponding locations.

V.6.5 Test FRFC 3A

Tested fire resistance: 56 minutes
Temperatures: Figure A2.30 and Figure A2.31- Appendix 2
Axial deformation: Figure A2.32- Appendix 2
Lateral deflection at midheight: Figure A2.33- Appendix 2
Observations: The column failed due to overall buckling toward the old part of the furnace. No local buckling of the external steel tube was observed. In some periods of the test, temperatures readings from four thermocouples (Th6, Th17, Th5 and Th4) were not reliable because they differed much from the average temperatures of other thermocouples at the same corresponding locations. The strain gauges were protected from heating (Figure V-11) but observations after the test show that the gauges were burned quickly by hot temperatures from the external steel tube, but not from the high temperatures in the furnace. Strain measurements (Figure A2.34) showed unappropriate results: strain at back side is higher than strain at front side while the column buckles toward the back side. Therefore, the strain measurements during fire test can not be accepted because of the damages at high temperatures of the strain gauges.

V.6.6 Test FRFC 3B

Tested fire resistance: 64 minutes
Temperatures: Figure A2.39 and Figure A2.40- Appendix 2
Axial deformation: Figure A2.42- Appendix 2
Lateral deflection at midheight: Figure A2.43- Appendix 2
Observations: Test FRFC 3B is the column with intumescent paint. The column failed due to overall buckling toward the old part of the furnace. Temperatures readings from thermocouple Th13 were not reliable because they differed much from the average temperatures of other thermocouples at the same corresponding locations. The intumescent painted layer starts

swelling at high temperature (about 200°C to 300°C). The expanded painted layer acts as a thermal barrier that effectively protects the column against rapid increase of temperature. The paint thickness measured after the test is between 12.5 and 14.0 mm. There were many cracks on the painting layer and they were progressing with temperatures (Picture A2. 3). Temperatures measured at the external steel tube vary in a wide range (Figure A2.39).

V.6.7 Test FRFC 4A

Tested fire resistance: 39 minutes
Temperatures: Figure A2.48 and Figure A2.49 - Appendix 2
Axial deformation: Figure A2.50- Appendix 2
Lateral deflection at midheight: Figure A2.51- Appendix 2
Observations: The column failed due to the buckling toward the old part of the furnace (Picture A2.4). Some special events happened during the second halftime of the test, with some steel cracking noises from the furnace. As can be seen on Picture A2.5, it is due to the local buckling deformations that appeared just in the middle of the column.

V.6.8 Test FRFC 4B

Tested fire resistance: 79 minutes
Temperatures: Figure A2.55 to Figure A2.57 - Appendix 2
Axial deformation: Figure A2.58- Appendix 2
Lateral deflection at midheight: Figure A2.59- Appendix 2
Observations: Test FRFC 4B is a column with intumescent paint. The column failed due to the overall buckling toward the old part of the furnace (Picture A2.6). Temperatures readings from thermocouples Th13 and Th3 were not reliable because they dropped to very low values. The painted layer swelled at about 200°C to 300°C and then some cracks appeared which progressed with temperatures. As can be seen on the column after the test (Picture A2.6), some parts of the painted layer fell off. Temperatures measured at the external steel tube vary in a wide range especially after 30 minutes (Figure A2.55 and Figure A2.56). Local buckling of the external steel tube was observed. (Picture A2.7).

V.6.9 Test FRFC 5A

Tested fire resistance: 104 minutes
Temperatures: Figure A2.63 Figure A2.64- Appendix 2
Axial deformation: Figure A2.65- Appendix 2
Lateral deflection at midheight: Figure A2.66- Appendix 2
Observations: The column failed due to the overall buckling toward the old part of the furnace. Temperatures readings from thermocouple Th8 were not reliable because they reached too high values.

V.6.10 Test FRFC 5B

Tested fire resistance: 35 minutes
Temperatures: Figure A2.69 and Figure A2.70 - Appendix 2
Axial deformation: Figure A2.71 - Appendix 2

Lateral deflection at midheight: Figure A2.72- Appendix 2
Observations: The column failed due to the buckling toward the old part of the furnace. Local buckling deformation appeared on the upper half of the column, at 1200 mm from the top (Picture A2.8). For all tests the square plates at the two ends had been welded to the external steel tube before testing. But in this test, it can be seen that the upper square plate has separated from the steel tube during the test (Picture A2.9 and Picture A2.10). The external steel tube shortened more than the internal concrete core did. There were slips between external steel tube and the concrete core. This phenomenon is also observed by the movement of the marks in the concrete core at the steam vents (Picture A2.11.).

V.6.11 Profile 6

Tested duration: 100 minutes
Temperatures: Figure A2.78- Appendix 2
Observations: This test was only intended for verifying the thermal transfer in the cross-section. No load was applied (Picture A2.12). Observation of the upper end of the columns after the test showed slips between the external steel tube and the concrete core (Picture A2.13). The internal steel tube and the surrounding concrete were still in contact.

V.7 Simulations and evaluation

V.7.1 Thermal analysis

All columns have been simulated using SAFIR program with the main assumptions previously described in part II.2.3 except that the value of water content is 6% in weight according to the measurements.
Two columns: FRFC 3B and FRFC 4B are fire protected by intumescent paint. In the test, the intumescent painted layer starts swelling at high temperature (about 200°C to 300°C). The expanded painted layer acts as a thermal barrier that effectively protects the column against rapid increase of temperature. But it is impossible to measure the thickness of the layer during fire. Therefore, in simulation, it is assumed that the intumescent paint thickness remains unchanged with temperature (fixed at 1mm in calculations) while the characteristic value of thermal conductivity varies with temperature. The modified thermal conductivity of the painted layer was adjusted to get a good agreement between measured temperatures and simulated temperatures in the profile. According to the observations made during the test, there were many cracks in the painted layer and they were progressing with temperature. Therefore the modified thermal conductivity of the painted layer increases for temperatures higher than 700°C as shown in Figure V-13 and Figure V-14.

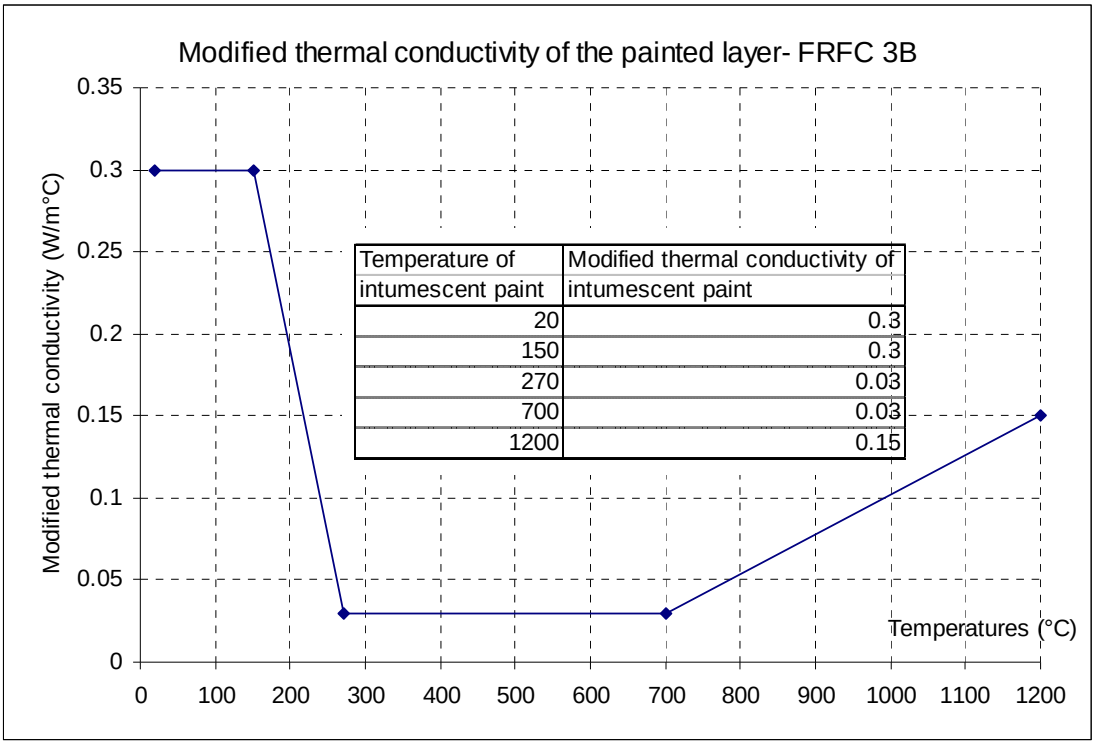

Figure V-13. Modified thermal conductivity of the painted layer of test FRFC 3B

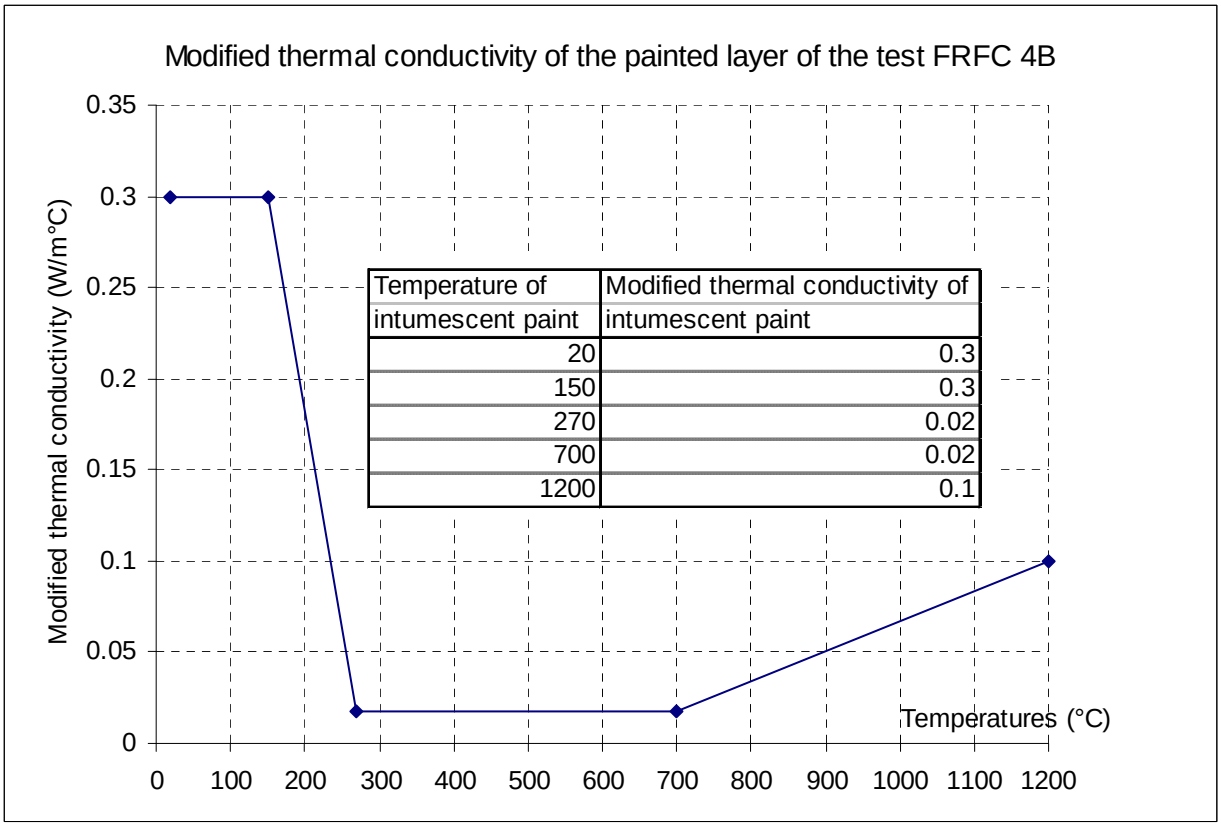

Figure V-14. Modified thermal conductivity of the painted layer of test FRFC 4B

Although the thickness of the painted layers in FRFC 3B and FRFC 4B are much different (column FRFC 3B was ~ 500 μm thick; column FRFC 4B was ~ 2000 μm thick but the global thermal conductivity of the two expanded layers does not differ much. As already mentioned, the increased modified thermal conductivity of the painted layer after 700°C is due to the damage of the product but the damage seems less important with a thicker painted layer.

Comparing the calculated and measured temperatures (showed in Appendix 2), the following comments can be drawn:

- Calculated temperatures on the external hollow section are in good agreement with the measured temperatures.
- There are systematic differences between calculated and measured temperatures in the internal steel profile: the measured vaporisation stage is longer than the simulated one; before the evaporation stage at the internal steel profile, the calculated temperatures are lower than the measured values. These differences can be explained by the migration of vapour in concrete (not taken into account in the model). In fact, part of this water moves to the external steel section, but can only escape through eight small holes generally drilled at the top and the bottom of the steel tube. Another part of the vapour migrates toward the coldest zones where it condenses again, which results in a slowing down of the vaporisation phase. Furthermore, when temperatures at the internal steel profile are lower than the values corresponding to the evaporation of free water, a part of hot vapour from the outer part of the section migrate to the inner part, and thus the temperature in the internal steel profile is somewhat higher than the value obtained by simulation. But these differences do not affect much the mechanical properties of materials because there is almost no decrease of the mechanical properties of steel and concrete at about 100°C to 150°C. In general, the temperatures in the internal steel profiles are simulated satisfactorily in all tests except in FRFC 6. Because columns FRFC 6 were tested at the young ages, it can be expected that the value of water content in concrete is higher than in other columns. Simulations with a value of water content in concrete of 9% have been done, and in this case, results show a good agreement (Figure A2.79 and Figure A2.80).
- With regard to the point inside the concrete, the agreement is not so good especially at low temperatures. Once more the difference between theoretical and experimental curves is primarily the result of the length of the vaporisation stage. Differences between theoretical and experimental curves do not affect much the variation of material properties: for low temperatures, the concrete mechanical properties are not affected and for higher temperatures, the agreement between theory and experiment is good enough.

V.7.2 Structural analysis

All columns have been simulated using SAFIR program with the main assumptions previously described in part III.3.2, except that the initial deflection of columns were adjusted based on the strain measurements at room temperature. For columns without strain measurements, the initial deflection of the column was chosen to get a satisfactory correlation between calculated and measured value of transversal displacement at midheight of the column.

In some tests, two strain gauges were attached for measuring the strains at two points. They are named back gauge and front gauge (Figure V-9). It can be seen in figures of Appendix 2 that the measured values always higher than the calculated values. It is guess that the real modulus of materials is higher then the calculated value. The average strains measured from back strain and front strain give the axial deformation of the column while the difference between back strain and front strain allow calculating the curvature and the lateral deflection of the column. Small variations of the modulus of materials do not affect much the deference between back strain and front strain. Therefore, for each column having strain measurements at room temperature, the initial deformation of the column, which is in fact unknown, is chosen to get a satisfactory correlation between calculated and measured value of the difference between back strain and front strain.

Another characteristic is also unknown. It is the relative position of the initial deflection in the furnace, since it can be situated in the direction of the old or of the new part of the furnace. Again numerical experimentation has been used to get the best correction between calculated and measured values and therefore define this position.

Measured transversal displacements of the moving beam that support the column indicate that the beam moves transversally at the beginning of the loading stage at room temperature (Figure V-15). It may be a rearrangement of position of the pin ends of the column. But during fire test, the beam did not move. Therefore, the measured displacements at room temperature can not be trusted, while the measured displacements during fire test can be used. The corrected displacement curve is the curve parallel to the measured curve. For vertical displacements, the moved measured value was obtained by translating the measured to get the same value at time 0 for the calculated curve and the moved measured curve. For transversal displacement, the measured curves were kept for clear vision but it is understood that the corrected curve is the curve parallel to the measured one.

Comparing the calculated displacements and measured ones (showed in Appendix 2), the following comments can be drawn:

- The calculated elongation of the columns is higher than the measured value in the first 5 minutes of testing. After this early stage, the calculated vertical displacements agree well with the measured values except for test FRFC 2A.
- The transversal displacement of the columns is sensitive to the assumed initial deformation.
- In all tests, after 2 to 4 minutes of fire, the column deforms toward the old part of the furnace and after some time toward the new part. This phenomenon does not appear in simulation if a uniform temperature around the column is adopted (Figure V-16). If the thermal gradient of temperatures in the furnace (as described in part V.4.2) is introduced, the calculated transversal displacement curve has the same form as the measured one (Figure V-17). The thermal gradient in the furnace is introduced by dividing temperatures in the furnace into two parts: one is the average measured temperatures in thermometers in the old part of the furnace, and one is the average value in the new part. All results

showed in Appendix 2 were calculated with the thermal gradient in the furnace. One sample is shown in Figure V-18. With this thermal gradient, the transversal displacement curve is not as smooth as the one corresponding to uniform temperatures. At some moments, the column changes its direction of deflection from the old part of the furnace to the new part or reverse. Therefore, the differences in the transversal displacement curves between the calculated results and measured results may be due to the gap between the real temperature field and the one chosen in the model.

- The measured transversal displacement at midheight of the column showed that the tested columns behaved in a relatively ductile manner. But in simulation, the columns failed in a less ductile manner: the transversal displacements change from small to large value in short time. These differences need to be explained. At high temperatures (over 400°C), carbon steels do not show strain hardening (EN 1993-1-2 (2005)) while in steel structures or composite steel-concrete structures without steel profile inside, the temperature in steel rises very quickly with time exposed to fire and it often higher than 400°C at the time column fails. Therefore, up to that moment, SAFIR uses the stress-strain relationship of the steel without strain hardening (detail in Appendix 1). But in the tested columns, the temperature in the internal steel profile during fire test is less than 400°C. It has been assumed that the strain hardening of the internal steel tube causes the ductility. A new model of material named STEELEC3SH was added to SAFIR program. The new model introduces the strain hardening of carbon steel at temperature below 400°C as indicated in Annex A - EN 1993-1-2 (2005). New simulations of the tested columns were made. But the result shows that all columns failed when the strains in steels are less than the strain value at the starting point of hardening stage (2%). Therefore, it can be concluded that the strain hardening of carbon steel does not affect the simulations.

- Another parameter should be considered. It is the confinement effects of the concrete core due to the steel tube which can cause the ductility of CFSHS columns. This assumption seems reasonable especially for columns with double tubes (profile 1, profile 2 and profile 5) because the internal steel tube does not degrade much during fire test, and thus it can confine the lateral expansion of concrete inside. Up to now, there are few research studies about the confinement effects on stress-strain relationship of concrete at high temperatures. It is believed that during fire, the external steel tube loses its stiffness and can not confine the concrete core much. Han L.H. deduced the stress-strain relations of concrete based on test results on concrete filled steel tubular axial short columns under constant high temperatures (Han L.H. (2001)). His model takes into account the composite action between the steel tube and the concrete core by introducing a constraining factor. A typical stress-strain relation for confined concrete of a concrete filled tube according to Han L.H. (2001) is shown in Figure V-19. Of course, in columns with double steel tubes, the constraining factor is different. Therefore, the study of the confining effects on concrete compressive strength at high temperature in CFSHS columns like those examined here could be a perspective of additional research works.

- In the tests, local buckling deformations of external steel were observed in some columns. This phenomenon is ignored in simulations. The question can then be raise whether the local buckling of the external steel affects much the global behaviour of the column. Analysing the stresses in external steel, it is seen that after only about 20 minutes in fire, the external steel looses almost all its strength so the load is transferred from the external steel to the concrete core. Therefore, it is believed that the local buckling of external steel tube affects little the fire resistance duration of the columns.

Comparison between the calculated and tested value of the fire resistance (Table V.4) shows that SAFIR program can predict well the fire resistance of self-compacting concrete filled steel hollow section columns provided properties of SCC are the same as those of normal vibrated concrete. In simulations shown in Appendix 2, the value and position of the initial deflection of columns were adjusted based on the strain measurements at room temperature of the columns and in order to get satisfactory correlations between calculated and measured value of transversal displacement at midheight of the column. All test columns have an initial deflection that does not exceed the value of L/500. It is therefore conservative to choose an initial deflection of L/500 cumulated with the eccentricity of loading.

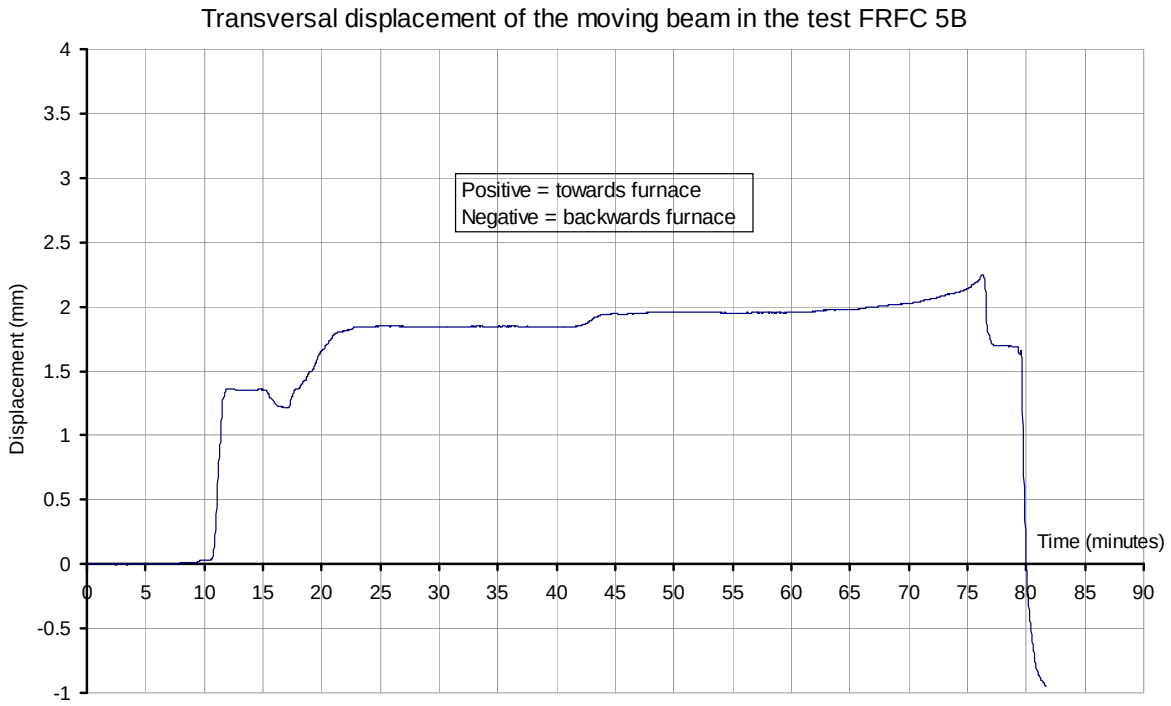

Figure V-15. Transversal displacement of the moving beam in the test FRFC 5B
(Loading stage from minute 10 to minute 24, fire stage from minute 41 to minute 76)

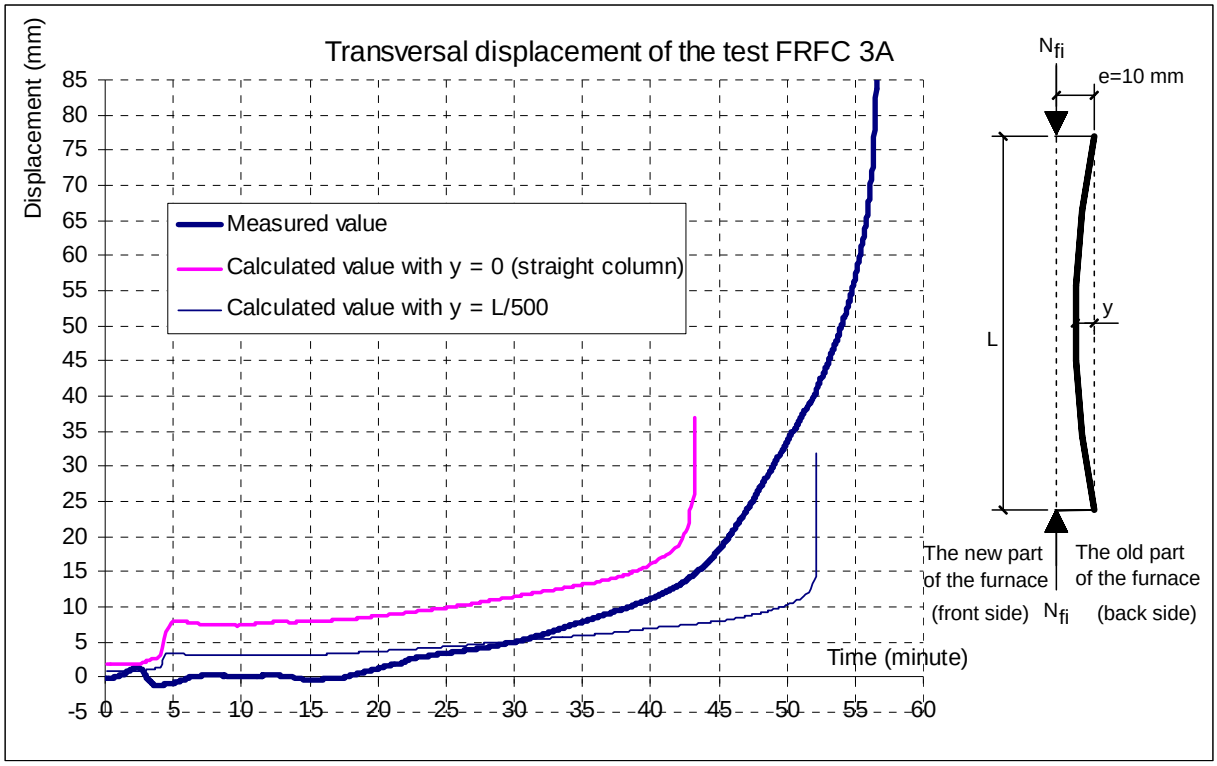

Figure V-16. Transversal displacement of the test FRFC 3A-
Calculated with average temperature in the furnace

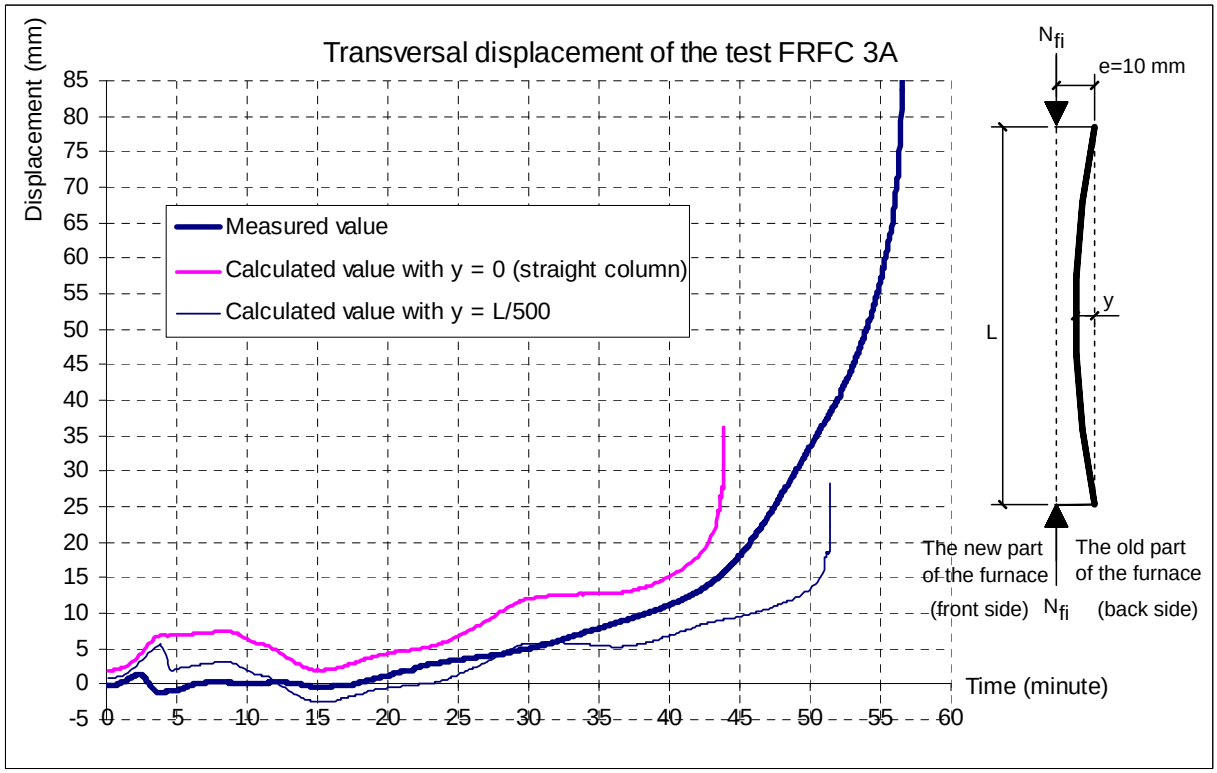

Figure V-17. Transversal displacement of the test FRFC 3A-
Calculated with thermal gradient between the old part and new part of the furnace

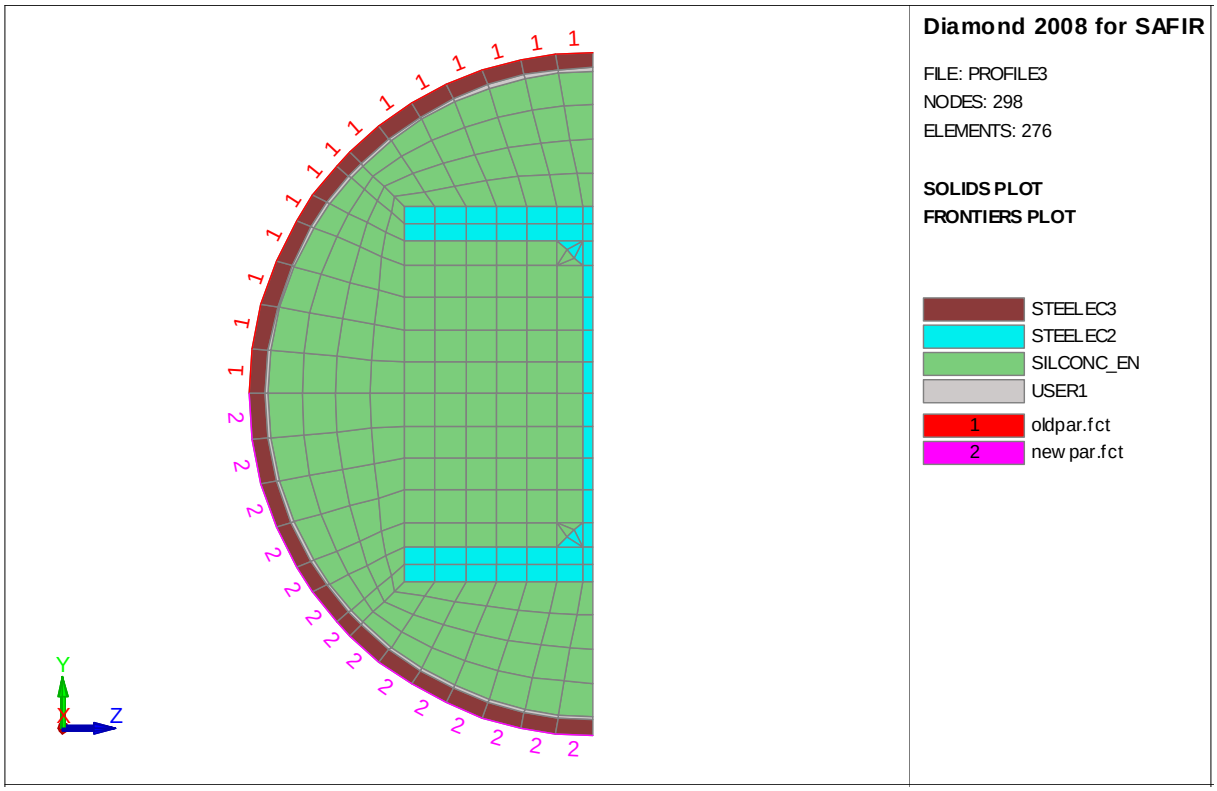

Figure V-18. Fire boundaries of a particular cross-section

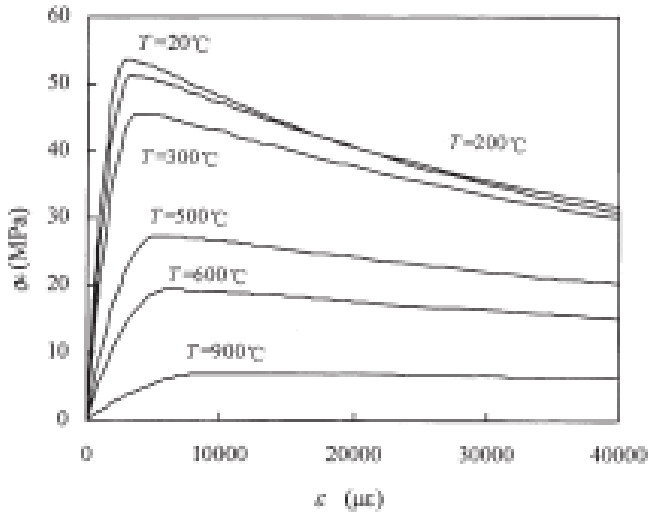

(a) Circular section

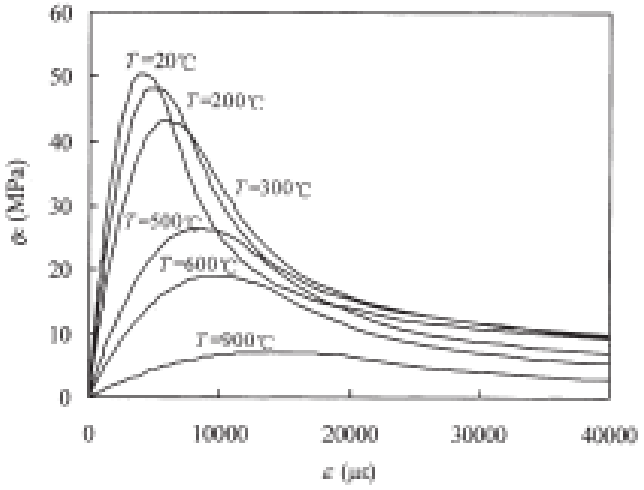

(b) Square section

Figure V-19. A typical stress-strain relation for confined concrete of a concrete filled tube according to Han L.H. (2001)

	Test load in fire		Load ratio	Tested	Calculated	
Test number	Load	Eccentricity		fire resistance	fire resistance	R_{t_cal}/R_{t_test}
	Nfi (KN)	e (mm)	Nfi/Nu	$R_{t\text{-}test}$ (minute)	R_{t_cal} (minute)	
Profile 1A	733	0	0.24	86	82	0.95
Profile 1B	1126	15	0.50	22	25	1.12
Profile 2A	688	15	0.30	65	67	1.03
Profile 2B	1244	10	0.50	43	41	0.94
Profile 3A	946	10	0.40	56	51	0.92
Profile 3B (with painting)	896	10	0.40	64	63	0.99
Profile 4A	1177	10	0.40	39	40	1.04
Profile 4B (with painting)	1124	10	0.40	79	73	0.92
Profile 5A	1199	10	0.30	104	87	0.84
Profile 5B	1998	10	0.50	35	41	1.16
					Mean =	0.99
					Standard deviation =	0.10

Table V.4 Comparison between calculated and measured fire resistance of tested columns

V.8 Conclusion

- SAFIR program can predict well the fire resistance of self-compacting concrete filled steel hollow section columns. In these simulations it has been assumed that the thermal and mechanical properties of SCC are very close to those of normal vibrated concrete. The results of the simulations corroborate this assumption.

    - There is an excellent agreement between calculated and test results regarding the values of the fire resistance.
    - For the axial and transversal displacements, the agreement can be considered rather good, but several adjustments had to be made, and the value of some unknown parameters had to be deduced from numerical experimentation.

- The assumptions (previously described in part III.3.2) used in simulations give conservative results. Therefore, it is suitable to use them to develop simplified methods for calculating the fire resistance of CFSHS columns. Simulations presented in chapter VI are based on these assumptions.